




Seismic hazard assessment for Iran in terms of macroseismic intensity

E. Shabani¹ · D. Albarello^{2,3}  · M. Mahsuli⁴ · N. Eghbali¹ · S. Hosseini Varzandeh⁴ · F. Farnetani²

Received: 2 March 2024 / Accepted: 17 June 2024 / Published online: 27 June 2024
© The Author(s) 2024

Abstract

We present the results of probabilistic seismic hazard assessment for Iran based on a statistical procedure specifically developed to manage macroseismic intensity data. This method takes into careful consideration the specific features of such data, which are characterized as ordinal, discrete, and confined within a finite interval, ensuring a logically coherent approach throughout the analysis. The results of our assessment are then compared with hazard maps generated using a standard approach, putting in evidence significant differences both on a national scale and relative to individual cities. This comparative analysis will be useful in identifying areas of utmost concern, where further studies are strongly recommended to yield hazard estimates of greater robustness and reliability. By pinpointing these critical scenarios, we aim to guide future research endeavors towards providing more accurate and reliable seismic hazard estimates. Identifying these critical situations facilitates the prioritization of resources and interventions, ultimately enhancing seismic risk mitigation efforts across Iran.

Keywords Seismic hazard · Macroseismic PSHA · SASHA · Macroseismic intensity · Disaggregation · Iran

1 Introduction

Seismic risk assessment, i.e., the expected loss due to the occurrence of a destructive earthquake, represents a basic tool for planning activities devoted to improving the resilience of communities where potentially damaging earthquakes may occur. In general, risk estimates require the combination of three main elements (e.g., Jena et al. 2020):

✉ D. Albarello
albarello@unisi.it

¹ Department of Seismology, Institute of Geophysics, University of Tehran, Tehran, Iran

² Department of Physics, Earth and Environmental Sciences, University of Siena, Siena, Italy

³ Institute of Environmental Geology and Geoengineering, National Research Council, Rome, Italy

⁴ Center for Infrastructure Sustainability and Resilience Research, Department of Civil Engineering, Sharif University of Technology, Tehran, Iran

seismic hazard (i.e., the level of expected ground shaking for a fixed future exposure period), vulnerability (i.e., the propensity of existing buildings to be damaged as an effect of the expected seismic ground shaking), and exposure (i.e., the amount and value of goods exposed to the earthquake). If all these elements are assumed to be known, a deterministic approach can be applied (e.g., Arslan Kelam et al. 2022). However, available information about these elements is far from exhaustive in developed countries, and the situation is even worse in developing countries.

Concerning seismic hazard, a mixture of physically and statistically based procedures are largely adopted around the world at global (e.g., Shedlock et al. 2000) and national (e.g., Rahimi and Mahsuli 2019) scales. Moreover, to provide realistic estimates, national-scale evaluations must be integrated with estimates of the effects that small-scale morpho-stratigraphic configurations may have on the expected ground motion (e.g., Jena et al. 2020).

Regarding vulnerability, deterministic and empirical approaches are also combined to determine fragility curves (Aguado et al. 2018; Del Gaudio et al. 2019; Chieffo et al. 2019; Dumova-Jovanoska 2000; Di Pasquale et al. 2005; Lagomarsino and Giovinazzi 2006; Fragiadakis and Diamantopoulos 2020; Martins and Silva 2021), which allow for the estimation of the impact that each level of ground shaking may have on buildings as a function of their configuration and structure. Finally, exposure estimates require an exhaustive evaluation of goods (e.g., concerning the stock of exposed buildings) classified in terms of respective vulnerability, which can be achieved only through rough statistical estimates or satellite imaging (e.g., Wieland et al. 2012).

The reliability of risk estimates provided by the above approaches relies on the amount and quality of available information, which is, in many cases and particularly in developing countries, quite unsatisfactory.

A different approach is proposed here, which can take advantage of the long-term historical documentation about the effects of past earthquakes available in many countries. This information is standardized by the use of macroseismic scales (e.g., Musson et al. 2010), which classify the impact of an earthquake on a settlement in terms of a finite number of scenarios of increasing severity. Thus, macroseismic estimates implicitly include all the elements involved in risk evaluations (seismic hazard, site effects, vulnerability of buildings, and exposure). Moreover, by considering sets of observables (including behavior of people, damages, etc.) and standardized elements (e.g., level of damages, gross vulnerability classes), macroseismic estimates can be provided by the analysis of historical documentary data in continuity with present-day observations.

Being qualitative (but not arbitrary) in character, macroseismic intensity evaluations cannot be used for anti-seismic design. However, they allow for a direct risk estimate, bypassing the difficulties arising when these estimates are performed in the standard way. Moreover, it allows for the exploitation of the large amount of data about the effects of past earthquakes, a heritage which is not considered in the standard approach except concerning the parametrization of seismic sources production rates. Additionally, macroseismic estimates can be easily understood by governmental bodies, stakeholders, and citizens, and thus are commonly used in risk communication (e.g., Saunders et al. 2022). Finally, macroseismic evaluations may help as a benchmark for probabilistic seismic hazard analysis (PSHA) carried out with standard procedures (e.g., Mucciarelli et al. 2008; Salditch et al. 2024). However, dealing with such a peculiar dimension (which is discrete, ordinal, and defined over a finite scale) requires specific procedures to manage relevant uncertainty relative to historical records.

To this purpose, D’Amico and Albarello (2008) introduced a statistical approach, referred to as SASHA (Site Approach to Seismic Hazard Assessment) to assess seismic hazard based on macroseismic intensity. This approach considers the specific characteristics of intensity data. This approach is tailored to handle uncertainties in historical earthquake data and lacks reliance on specific seismic models. While comparisons with existing hazard estimates reveal differences, emphasizing the need for further refinement, the primary focus is on using historical seismicity to provide a baseline for hazard assessment. SASHA has been effectively utilized for seismic hazard assessment in various countries, including applications highlighted by Gómez Capera et al. (2010), Bindi et al. (2012), Ullah et al. (2015), D’Amico et al. (2016), and Jimenez et al. (2016).

In this context, we present an application pertinent to Iran. The primary features of the SASHA procedure are briefly outlined at first, the description of the intensity data utilized in the procedure is provided. Finally, SASHA results are compared with independent hazard estimates available for Iran, as provided by Hosseini Varzandeh and Mahsuli (2023a, b), which employ a different approach. The goal is not to discredit existing methods but to provide a possible benchmark and gain new insights about the reliability of available seismic hazard and risk estimates in Iran.

2 The SASHA approach

The SASHA approach is fundamentally phenomenological, relying on statistical analysis of sequences of intensity data at a specific site. This method consists of two main steps. Firstly, the local seismic history, which represents the sequence of intensity values reflecting the local effects of past earthquakes is reconstructed utilizing available information and considering relevant uncertainties. This involves merging effects documented at the site with those inferred from epicentral information using appropriate attenuation relationships in a probabilistic manner to generate a comprehensive local seismic history. To incorporate relevant uncertainties, each seismic occurrence at time t is characterized by a discrete probability distribution, $P_t(\geq I)$, which indicates the probability of effects corresponding to intensity 'I' or greater during the earthquake. By considering the entire set of 'M' known events, the expected number, $\bar{N}_j(\geq I)$, of events occurring during any time interval Δt_j is computed in the following form:

$$\bar{N}_j(\geq I) = \sum_{t \in \Delta t_j} P_t(\geq I). \tag{1}$$

These estimates are used to evaluate the statistical completeness of the catalogue by following the methodology outlined by Albarello et al. (2001). The probability $Q_j(\geq I)$ that at least one event has occurred with $\geq I$ in the time span Δt_j , will be.

$$Q_j(\geq I) = 1 - \prod_{t \in \Delta t_j} [1 - P_t(\geq I)]. \tag{2}$$

The local seismic hazard $H_{\Delta t}(\geq I)$ relative to an exposure time Δt can be computed in the assumption that the seismogenic process is ergodic by using the relationship.

$$H_{\Delta t}(\geq I) = \frac{1}{K} \sum_{j=1}^K Q_j(\geq I) \tag{3}$$

where K is the number of non-overlapping intervals Δt_j , each of duration Δt , in the interval completeness for the local seismic records. It's important to note that no assumptions are made regarding the time distribution of events, thus obviating the need for after-shock removal when applying the procedure. Additionally, an appropriate approach can be employed to address uncertainty concerning catalog completeness and relevant statistics (for details, refer to D'Amico et al. 2008). Furthermore, based on Eq. (1), a deaggregation analysis can be conducted using the method outlined by Albarello (2012). Finally, employing suitable probabilistic conversion rules (Gómez Capera et al. 2020), the results of the SASHA procedure can be translated into ground-motion parameters, such as peak ground acceleration (PGA) and spectral acceleration (SA) at various vibration periods, while considering the uncertainty associated with this conversion (see D'Amico and Albarello 2008).

In summary, the SASHA procedure provides three kinds of outcomes: (1) hazard curve, i.e., the probability that an earthquake with an intensity not less than I_s will occur at the site during a given exposure time, for each threshold I_s ; (2): the reference intensity I_{ref} values (and respective SA and PGA values) are determined corresponding to a fixed probability threshold; (3): disaggregation results, i.e., magnitude/distance pairs more representative of I_{ref} and identification of the past earthquakes that are most important for the local hazard. Regarding outcome (2), it can also be provided upon request.

3 The Iranian context

The map in Fig. 1 illustrates active faults in Iran as compiled by Hessami et al (2003). Following the classification by Mirzaei et al. (1998), Iran is categorized into five primary seismotectonic regions: Alborz-Azarbayejan, Central-East Iran, Kopeh Dagh, Makran, and Zagros (Fig. 1).

Typically, recent seismicity data indicate b-values that within the majority of these areas ranges between 0.9 and 1.0. Notably, the Zagros region exhibits the highest b-value, ranging from 0.98 to 1.16, while the Makran seismotectonic zone demonstrates the lowest values, ranging from 0.67 to 0.75 (Mousavi Bafrouei and Mahani 2020). Consequently, it's unsurprising that Iran's most notable recorded earthquake occurred in the Makran subduction zone, measuring a magnitude of 8.1 (Ambraseys 2001).

As concerns historical data, the majority of intensity reports for Iran have been documented by Berberian (1976a, b, c, 1977, 1981, 2005) using the MMI scale, by Ambraseys and Melville (1982) with the AMS scale, and by Ambraseys (2001) employing the MSK scale. Amini et al. (2017) reconciled intensity values from various authors across different scales to create a unified dataset of Iranian earthquakes. This involved a comprehensive review, drawing information from diverse sources such as books, articles, and reports from esteemed institutions including the International Institute of Earthquake Engineering and Seismology (IIEES), the Building and Housing Research Center (BHRC), the Geological Survey of Iran (GSI), and the National Geoscience Database of Iran (NGDIR). The primary sources for macroseismic data on Iranian earthquakes were field studies conducted by Ambraseys, Berberian, and their collaborators, regarded as the most reliable. The dataset encompassed approximately 350 earthquakes with descriptions, some accompanied by intensity values, and about 150 earthquakes solely characterized by intensity values, lacking accompanying descriptions. Amini et al. (2017) compiled intensity values for 512 Iranian earthquakes and provided corresponding epicentral information, including timing details (Year,

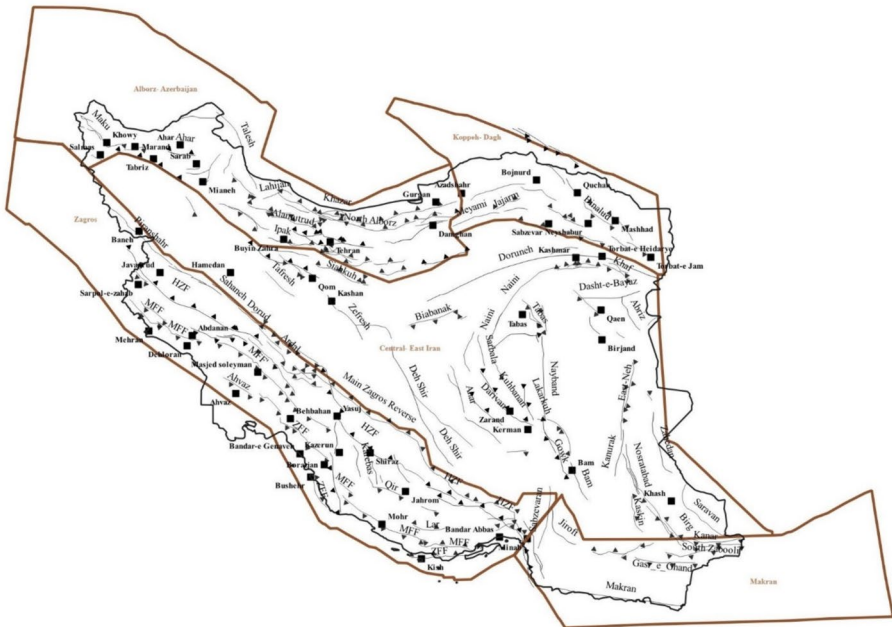


Fig. 1 The map illustrates active fault lines in Iran, sourced from Hessami et al (2003). The primary seismic-tectonic regions within Iran have been delineated, based on the classification by Mirzaei et al. (1998)

Month, Day), presumed epicentral location, macroseismic Magnitude (M_w), and epicentral Intensity based on EMS (European Macroseismic Scale by Grünthal 1998), ESI (environmental macroseismic scale by Guerrieri et al. 2015) eventually jointly considered (EMS–ESI scale). All events in the dataset were assigned intensity values according to the EMS–ESI scale. However, for earthquakes with descriptions of building damage and environmental effects, the EMS and ESI scales were reassessed. A conversion from a 5-degree scale to a 12-degree scale was carried out using uniform intensity scales. The dataset covered the period from 658 to 2013, with intensity values ranging from IV to XI EMS. There may be concerns about comparing the effects of earthquakes over long time intervals, given the significant variations in the vulnerability of settlements. However, macroseismic intensity scales (e.g., the EMS scale used in the paper) account for differences in building vulnerability, enabling the comparison of intensities from events impacting different settlements over time. Additionally, in the case of Iran, as mentioned in the paper by Amini et al. (2017), intensity estimates have been revised to eliminate potential biases. This does not imply that the accuracy level remains constant over time, but rather that no bias is expected due to the varying exposure levels at the examined sites.

For this study, events with magnitudes equal to or greater than 5.5 were selected, totaling 339 events with $M_w \geq 5.5$ sourced from the catalog compiled by Amini et al. (2017). Additionally, parameters for 25 events occurring between 2014 and May 2023 were collected and included. Thus, a total of 364 events were analyzed in this study (see Appendix 1). Figure 2 illustrates the epicenters of earthquakes from the Iranian catalog with $M_w \geq 5.5$ up to March 2023.

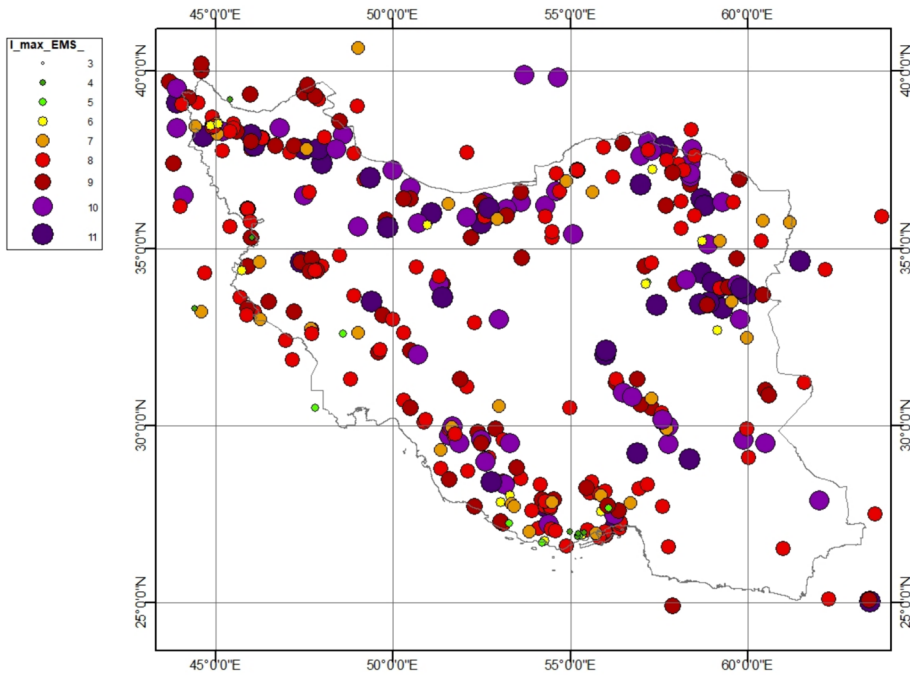


Fig. 2 The epicentral locations of the seismic events considered in the present study. Colors and sizes of the symbols differentiate events based on the estimated epicentral intensity

4 Selecting intensity attenuation models

Local seismic histories required for the SASHA approach were often unavailable or incomplete, especially for minor towns, hindering their incorporation into hazard estimates. Instead, these histories were reconstructed using epicentral data, with consideration given to available attenuation relationships.

Typically, attenuation relationships are expressed in terms of recorded ground-motion parameters. Several studies have aimed to derive intensity attenuation relationships specifically for Iran. Chandra et al. (1979) developed a model based on isoseismal maps of ten earthquakes occurring in Iran between 1957 and 1977. Ambraseys and Melville (1982) formulated their model using 82 isoseismal lines from 26 earthquakes prior to 1900. More recent contributions include Ahmadzadeh et al. (2019), Yaghmaei-Sabegh (2018), Zare (2017), and Moradi et al. (2004). Ahmadzadeh et al. (2019) evaluated a relation using isoseismal maps from 31 earthquakes with magnitudes ranging from 5.1 to 7.4, occurring between 1939 and 2017. Zare (2017) focused on linking intensity to peak ground acceleration, primarily utilizing macroseismic intensity data relative to earthquake magnitude. Yaghmaei-Sabegh (2018) predicted macroseismic intensity attenuation using data ranging from 4.1 to 7.4 in magnitude, collected from 1975 to 2013. However, according to Ahmadzadeh et al. (2019), the studies of Zare (2017) and Yaghmaei-Sabegh (2018) included small earthquakes, leading to potentially problematic intensity estimations based on observations of damage to rural buildings in the meioseismal regions, resulting in significant uncertainties. Hence, their outcomes were not considered in the present study.

Moradi et al. (2004) provided macroseismic intensity attenuation models for Iran based on data from 22 earthquakes, comprising over 105 isoseismal intensity maps for specific magnitudes. They presented attenuation relationships along the fault direction, perpendicular to it, and an average relationship. In this study, the attenuation models by Ahmadzadeh et al. (2019) and Moradi et al. (2004), as reported in Table 1, were initially considered.

To determine the most effective attenuation model, we considered the maximum recorded intensities (I_{max}) spanning 50 years (1973–2023) across different towns (as shown in Table 2). These locations were strategically chosen to encompass a broad area of Iran, ensuring an adequate geographical spread to confirm that the observed I_{max} values were not influenced by the same earthquake. This allows us to treat them as independent manifestations of a stochastic process.

The SASHA approach was employed to generate two alternative hazard estimates by considering the two models presented in Table 1. Consequently, using equation [3], two estimates of the probability $H_{\Delta t}^i(\geq I_{max}|Model)$ were obtained at each i -th site, indicating the likelihood that the respective I_{max} intensity would be reached or exceeded within a 50-year period ($\Delta t=50$). Two sets of values $H_{50}^i(\geq I_{max}|1)$ and $H_{50}^i(\geq I_{max}|2)$ were assessed for each site, corresponding to Model 1 and Model 2 in Table 1, respectively. For each model, two likelihood estimates, l_1 and l_2 , were computed by considering all N sites in Table 2:

$$l_1 = \ln \left\{ \prod_i^N H_{50}^i(\geq I_{max}|1) [1 - H_{50}^i(\geq I_{max}|1)] \right\} \tag{4a}$$

$$l_2 = \ln \left\{ \prod_i^N H_{50}^i(\geq I_{max}|2) [1 - H_{50}^i(\geq I_{max}|2)] \right\}. \tag{4b}$$

The log-likelihoods relative to Models 1 and 2 resulted $l_1 = -314$ and $l_2 = -142$ respectively. Since Model 2 maximizes the likelihood, it can be considered the best performing one and used in the following to estimate seismic hazard in terms of macroseismic intensity in Iran.

5 Seismic hazard maps in Intensity

Seismic hazard was assessed across Iran by considering a uniform grid system. Utilizing the SASHA method and taking into account attenuation Model 2, the seismic hazard was quantified in reference to a 10% likelihood of surpassing a certain intensity (I_{ref}) within a 50-year timeframe, corresponding to an average return period of 475 years in the standard Poissonian model (Fig. 3). As anticipated, the resulting pattern closely mirrors the occurrence distribution of significant seismic events documented in the area.

The disaggregation analysis also facilitated the identification of the earthquake most influential in the local hazard, a particularly relevant aspect for Tehran. This city has been scrutinized by Hosseini Varzandeh and Mahsuli (2023a). According to the SASHA analysis, Tehran exhibits a relatively low seismic hazard, with an intensity level reaching only VI, characterized by a 10% exceedance probability within 50 years. This is the highest intensity value observed in Tehran including the most recent event (2017; $M_w=4.9$; $I_{max}=VI$). This outcome may be surprising given the proximity to long

Table 1 Intensity Attenuation models considered in this study

Model	Name	Relationship	Explanations
1	Ahmadzadeh et al. (2019)	$I = -0.841 + 1.583M_w - 1.344 \ln \sqrt{R_{epi}^2 + h^2} - 0.0027 \sqrt{R_{epi}^2 + h^2}$	$h = 5.92\text{km}$ and the standard deviation is $\sigma = 0.68$ (Macroseismic data of Iran)
2	Moradi et al. (2004)	$I = 0.554I_0 + 12.757 - 2.7\log(R + 22)$	$R < 167\text{km}$ and $\sigma = 0.49$ (Macroseismic data of Iran)

Table 2 Observed maximum intensities at 50 main towns and corresponding maximum observed intensities (I_{max}) in the time span 1973–2023. $H(I_{max})$ indicate the probabilities computed by the SASHA approach that the observed I_{max} value is expected to be reached or exceeded in a time span of 50y

Locality	Model 1				Model 2			
	Lat (°N)	Lon (°E)	I_{max}	$H(I_{max})$	Lat (°N)	Lon (°E)	I_{max}	$H(I_{max})$
Abdanan	32.99	47.41	6	0.000	38.55	44.95	8	0.000
Ahar	38.48	47.07	8	0.000	26.56	54.02	5	0.010
Ahvaz	31.32	48.67	<4	0.010	38.43	45.77	<4	0.206
Azadshahr	37.09	55.17	5	0.106	36.30	59.60	<4	0.141
Bam	29.11	58.36	11	0.000	31.94	49.30	7	0.000
Bandar Abbas	27.18	56.27	9	0.000	33.12	46.16	8	0.000
Bandar-e Genaveh	29.58	50.52	9	0.000	37.42	47.72	8	0.000
Baneh	36.00	45.89	<4	0.038	27.14	57.07	5	0.020
Behbahan	30.60	50.24	<4	0.020	27.55	52.88	7	0.000
Birjand	32.87	59.22	6	0.010	36.22	58.82	<4	0.166
Bojnurd	37.48	57.33	8	0.000	33.73	59.19	7	0.020
Borazjan	29.27	51.22	7	0.000	34.64	50.88	5	0.038
Buyin Zahra	35.77	50.05	5	0.154	37.11	58.51	<4	0.240
Bushehr	28.91	50.83	<4	0.000	36.21	57.68	<4	0.074
Damghan	36.17	54.35	5	0.106	38.20	44.77	7	0.120
Dehloran	32.69	47.27	8	0.000	37.94	47.54	7	0.010
Gorgan	36.84	54.43	<4	0.098	34.46	45.86	8	0.000
Hamedan	34.81	48.52	<4	0.038	29.61	52.54	<4	0.236
Jahrom	28.50	53.56	<4	0.160	33.60	56.92	5	0.065
Javanrud	34.81	46.49	6	0.000	38.08	46.30	<4	0.218
Kashan	33.98	51.43	<4	0.154	35.69	51.39	6	0.020
Kashmar	35.24	58.47	<4	0.048	35.27	59.22	4	0.141

Table 2 (continued)

Locality	Model 1			Model 2			Model 1			Model 2		
	Lat (°N)	Lon (°E)	I _{max}	H(I _{max})	I _{max}	H(I _{max})	Lat (°N)	Lon (°E)	I _{max}	H(I _{max})	I _{max}	H(I _{max})
Kazerun	29.62	51.65	5	0.250	5	0.090	35.24	60.62	7	0.000	7	0.010
Kerman	30.28	57.08	6	0.000	6	0.120	30.67	51.59	8	0.000	8	0.000
Khash	28.22	61.22	8	0.000	8	0.000	30.81	56.56	6	0.020	6	0.192

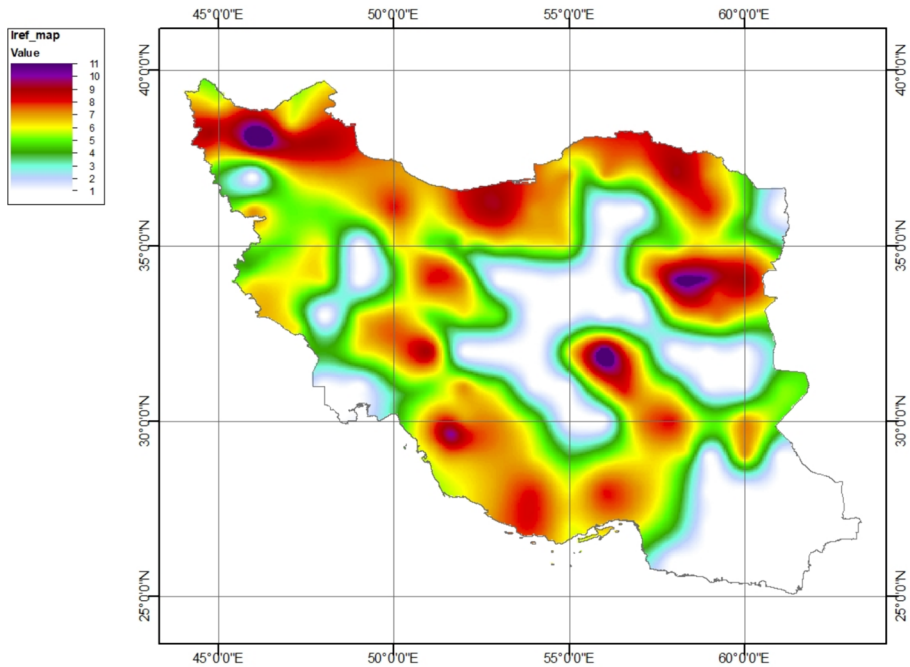


Fig. 3 The seismic hazard map of Iran is depicted relative to intensity values associated with a 10% probability of exceedance in 50 years, corresponding to an average return time of 475 years in the Poisson model

fault lines that could potentially cause strong earthquakes. However, Berberian and Yeats (2016) noted that no medium- to large-magnitude earthquakes (M_w 6.5–7.5) have occurred within the Tehran metropolitan region over the past 839 years along the faults beneath or near the metropolitan area. This suggests that the seismic activity rates of these faults are very low, with expected return times for large earthquakes spanning thousands of years and thus with a low probability of occurrence during a time span of tens of years (which is the target of the present hazard analysis). In line with this hypothesis, paleo-seismological researches by Ritz et al. (2006, 2012) revealed that the North Tehran fault has secondary active fold-and-thrust structures and a reverse fault, with evidence of eight significant seismic events ($M_w > 6.5$) over the past 30,000 years, suggesting a recurrence interval of 3200–4100 years. The Taleghan fault has experienced 2–3 events ($M_w \geq 7$) in the last 3500 years, with a recurrence interval of 1200–1800 years. The Moshafault showed evidence of several ground ruptures in the past 10,000 years, with significant events ($M_w > 7$) recurring every 1200–1600 years.

The SASHA approach also enables the identification of historical events responsible for estimated hazard (Fig. 4). Epicenters of these events are represented in Fig. 5, with symbols that scale according to their relative contributions to the seismic hazard in Tehran. It's notable that most of the contribution stems from ancient events (e.g. 958 AD and 1177 AD). According to the attenuation relationship utilized in this study, the highest intensity estimated at the city center is intensity VIII, corresponding to the event in 958 AD.

According to reevaluations made by Berberian and Yeats (2016), the latest earthquake to affect the present Tehran metropolitan area was the Lavāsānāt earthquake on

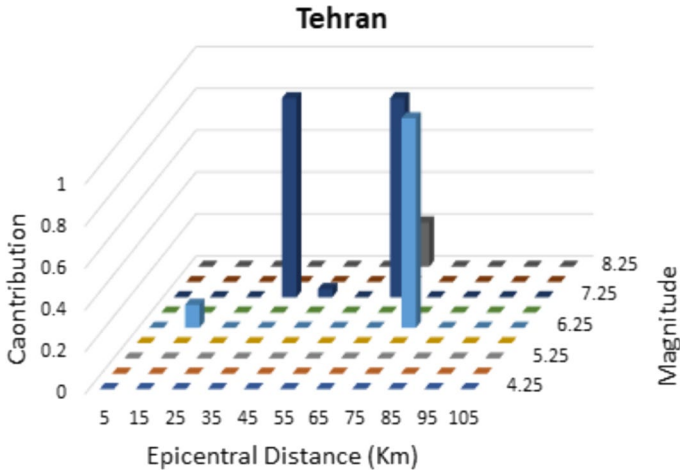


Fig. 4 Hazard disaggregation plot relative to Tehran for an exceedance probability of 10% and an exposure time of 50 years. Bars are proportional to the contribution of the respective magnitude/distance pairs to seismic hazard

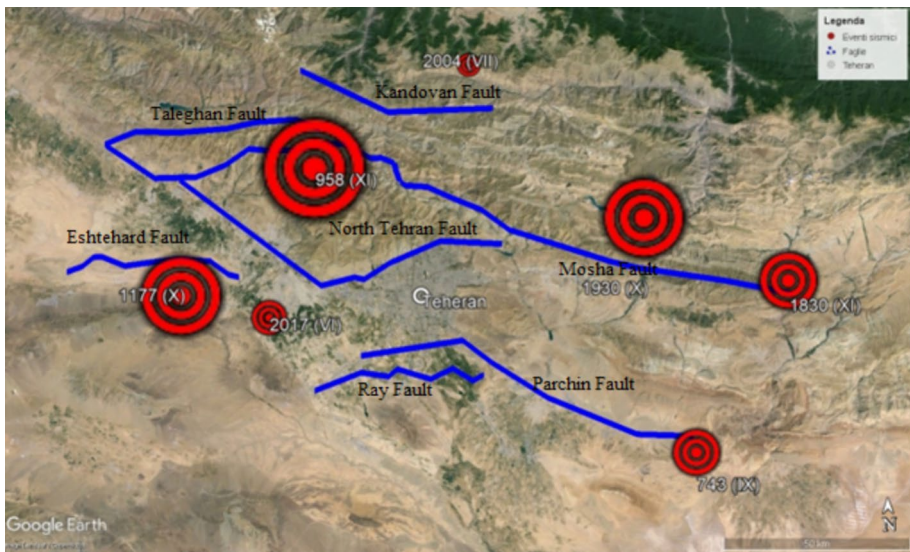


Fig. 5 Outcome of the disaggregation analysis relative to Tehran for an exceedance probability of 10% in 50y. The red circles identify epicentral location of historical events responsible for seismic hazard at the site. The size of the circle is proportional to the contribution provided by the respective event. For each earthquake, the year of occurrence and the epicentral intensity are also reported. Blue lines trace the faults reported by Hessami et al (2003))

the central section of the Moshā fault, on 27 March 1830, with its epicenter located ~ 30 km northeast of the city, which had a magnitude of $M_w \sim 7.0\text{--}7.4$; prior to that, the Ruyān earthquake north of Tehran struck the same section of the fault on 23 February

958, with a reevaluated magnitude around $M_w \geq 7.0$ (7.0–7.4). Additionally, these Authors suggest that the North Tehran fault system west of Tehran experienced an earthquake of $M_w \sim 7.0$ in May 1177. Apart from the 1830 earthquake, no medium- to large-magnitude earthquakes (M_w 6.5–7.5) have occurred within the Tehran metropolitan area over the past 839 years along the faults beneath the metropolitan area or its immediate vicinity.

6 Comparing SASHA outcomes with existing hazard maps of Iran

No seismic hazard map for Iran has been published in terms of macroseismic intensity. However, several maps have been generated based on Peak Ground Acceleration (PGA). Following the map provided by Mousavi et al. (2014), Hosseini Varzandeh and Mahsuli (2023a, b) published a new map. Their methodology relied on probabilistic seismic hazard analysis using the structural reliability method, previously introduced by Rahimi and Mahsuli (2019), Mahsuli et al. (2019) and Askari and Mahsuli (2020), where a comprehensive review of earlier attempts can be found. They produced nationwide hazard maps for PGA as well as spectral accelerations. As depicted in Fig. 6, they illustrated that large areas of Iran have moderate PGA values up to 0.24g, while PGA exceeds a stringent threshold of 0.6g in certain restricted areas.

Similarly, Mousavi Bafrouei et al. (2014) examined seismic hazard zoning in Iran. They identified the highest hazard level for earthquake events occurring along the Zagros Main

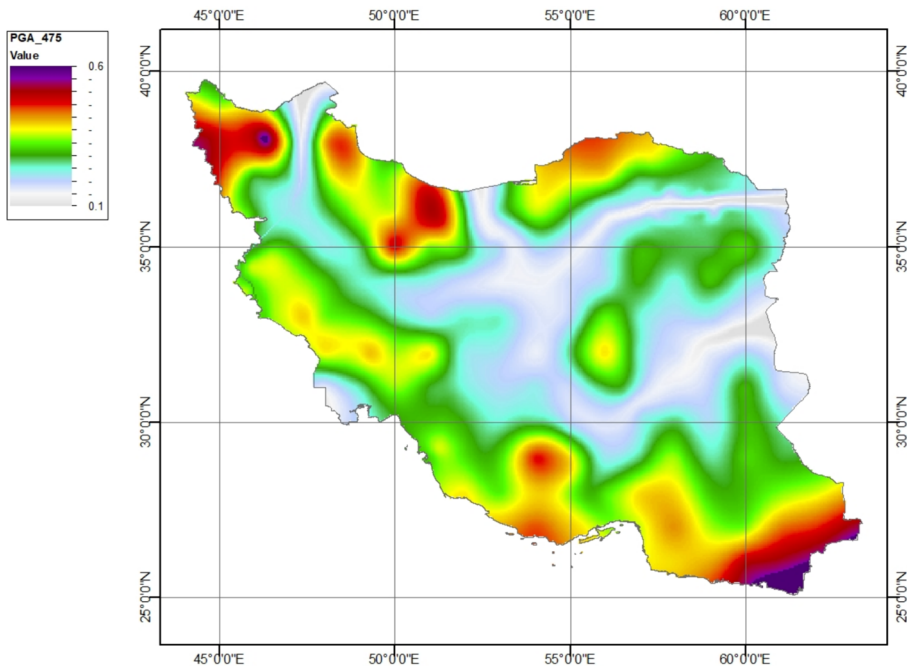


Fig. 6 Seismic hazard map of Iran in terms of PGA (fraction of gravity acceleration, g) by Hosseini Varzandeh and Mahsuli (2023a)

Recent Fault (MRF), particularly in parts of Lorestan and Kermanshah provinces in the west of the country (Fig. 1). The lowest estimated hazard levels are primarily associated with the Lut block (Fig. 1) in the east and central regions of the country, notably Yazd and Isfahan provinces.

Both hazard maps in Figs. 3 and 6 represent seismic hazard over the same exposure interval under the assumption that seismicity follows a stationary stochastic process. In both cases, ground motion attenuation relationships and historical seismicity are crucial for parameterizing the underlying computational model. Additionally, both methods aim at addressing both epistemic and aleatory uncertainty. However, there are inherent differences between them. Beyond statistical technicalities, the SASHA approach is purely phenomenological, a characteristic also presents in the model proposed by Hosseini Varzandeh and Mahsuli (2023a). While this difference could be seen as a limitation, it's essential to note that seismotectonic zoning considered in the model by Hosseini Varzandeh and Mahsuli (2023a) involves high uncertainty, which can significantly impact final hazard outcomes. The SASHA approach strictly relies on historical seismicity, which represents fundamental information given the time span covered by this data. In this regard, the SASHA outcome could be considered a basic benchmark, as hazard outcomes should align with seismicity observed in the recent past.

Nonetheless, a comparison could help identify potential limitations of both approaches. Directly comparing the estimates in Figs. 2 and 6 isn't feasible as they pertain to different parameters. However, both estimates provide a ranking of sites in terms of seismic hazard. This ranking could serve as the basis for comparison (e.g., Mucciarelli et al. 2008). To this end, two new maps have been prepared where a rank has been assigned to each node of a regular grid covering the country. These ranks reflect the relative position of each node when ordered in terms of hazard.

The comparison of the hazard maps is presented in Fig. 7 in terms of ranks for an exceedance probability of 10% over a 50-year period. The map on the left shows the estimates derived using the SASHA approach, while the map on the right displays the estimates provided by Hosseini Varzandeh and Mahsuli (2023a).

The two maps exhibit clear similarities, such as the high seismic hazard levels along the northern and southwestern boundaries of Iran. However, significant discrepancies are also evident in many regions of the country, such as in the Makran and northwestern

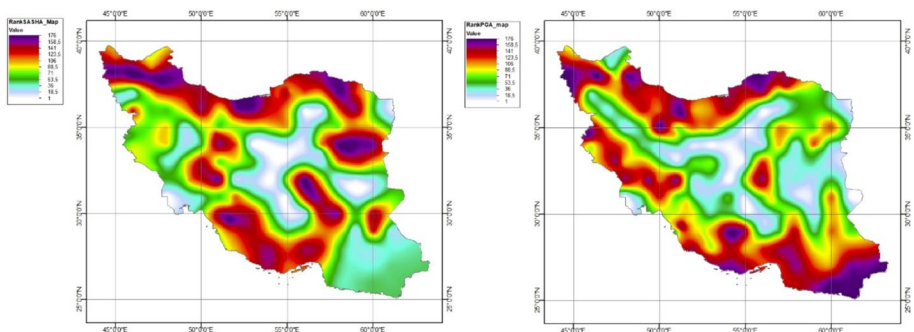


Fig. 7 Comparison of the hazard maps in terms of ranks relative to an exceedance probability of 10% in 50y. On the left the estimates by the SASHA approach, on the right the ones by Hosseini Varzandeh and Mahsuli (2023a)

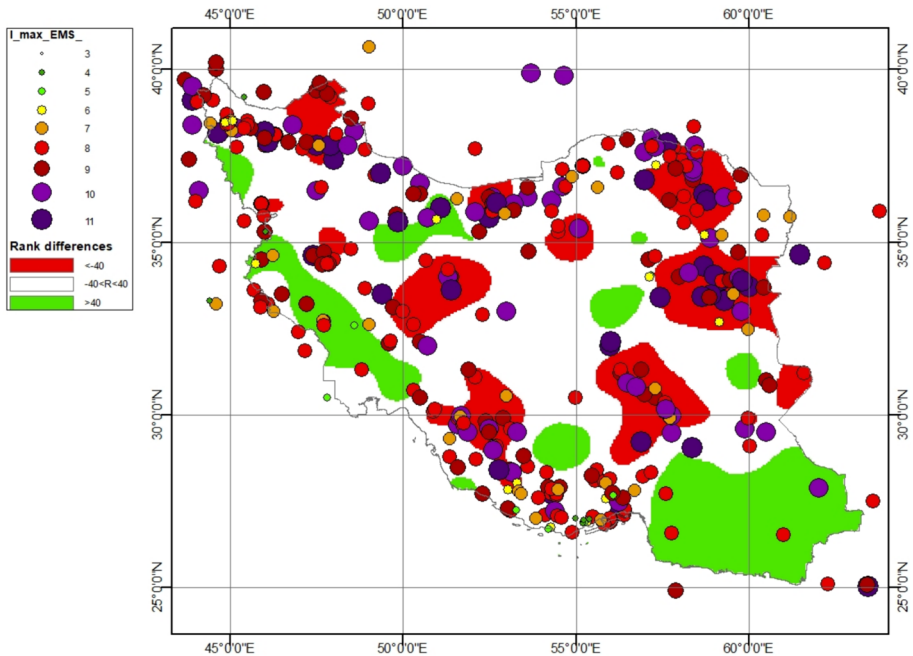


Fig. 8 Significant Rank differences in hazard estimates between SASHA and Hosseini Varzandeh and Mahsuli (2023a). Red indicates SASHA's estimates are the highest; green indicates the opposite. Epicenters of historical earthquakes are also reported for reference: colors indicate the respective I_{max} value

part of the Zagros zones. To better understand these differences, Fig. 8 presents rank differences along with the epicenters of historical events, providing a clearer view of the observed differences. This figure illustrates the ranking differences in hazard estimates between SASHA and Hosseini Varzandeh and Mahsuli (2023a). In particular, by considering the whole set of rank differences, those in the range between the first and third quartile were not considered as significant in that both approaches provide similar results. Negative differences (in red in Fig. 8), indicate that SASHA's estimates are the highest, while positive differences (in green in Fig. 8) indicate the opposite.

One noticeable trend is that where historical events are concentrated (e.g., along the northeastern border of Iran), SASHA tends to provide relatively higher estimates compared to those presented by Hosseini Varzandeh and Mahsuli (2023a) (see Table A2-1). This discrepancy could be attributed to seismotectonic zoning (Mucciarelli et al. 2008). In fact, when seismotectonic zones are delineated, it is assumed that seismic activity is evenly distributed across the entire zone. However, this can lead to an artificial reduction in observed seismic rates per unit area if earthquakes occur only in specific parts of the zone. This assumption may be accurate if the size of the seismogenic area is precisely estimated, otherwise, this could result in a significant underestimate of the actual seismic potential. Conversely, if the size of the seismogenic area is underestimated, it could result in higher hazard estimates. This might be the case in the southernmost part of Iran (Makran), where SASHA provides relatively low hazard values due to the lack of significant historical events in the area. Alternatively, it could be argued that seismotectonic zoning might incorporate historical data, which could be potentially

incomplete. Determining the likelihood of each map would necessitate a thorough analysis on a case-by-case basis.

In the Iranian segment of the Makran subduction zone, no significant thrust fault earthquakes have been documented, and there no interplate seismic activity is currently recorded (Penney et al. 2017; Abbasi et al. 2024; Aghdam et al. 2024). Byrne et al. (1992) observed a distinct segmentation zone in seismic behavior between the eastern and western parts of the Makran zone. In the eastern segment, located in Pakistan, significant thrust earthquakes have been historically recorded, such as the great (Mw 8.1) earthquake of 1945, along with ongoing occurrences of smaller to moderate-sized thrust earthquakes. In contrast, the western segment, the Iranian part, lacks documentation of major earthquakes in historical records, and modern instrumentation has not detected many shallow events along the plate boundary in this region. Their findings indicate that aseismic conditions persist at depths shallower than approximately 17 km along the shallowest 70–80 km of the plate boundary, spanning the entire margin.

Regarding the specific case of Tehran, SASHA provides a reference intensity of VI, corresponding to a PGA value of 0.4g proposed by Hosseini Varzandeh and Mahsuli (2023a). A significant difference between the disaggregation provided by the approach of Hosseini Varzandeh and Mahsuli (2023a) and SASHA is that in the latter case, the focus is on single specific events, while the former focuses on the expected (assumed) seismogenic structures.

7 Discussion and conclusion

A new hazard map of Iran has been proposed in terms of macroseismic intensity, which can aid in a preliminary assessment of seismic risk by providing a more direct and understandable depiction of the expected social and economic impact of future earthquakes. The SASHA approach considered here has been tailored to manage the specific characteristics of macroseismic data, which are ordinal, discrete, and defined on a finite scale, while also accounting for uncertainty affecting relevant information, such as uncertain intensity for historical events and possible incompleteness of the historical record. Moreover, it is a purely phenomenological approach whose outcomes rely solely on the historical record at the study site and do not incorporate any seismotectonic information. In general, the SASHA was originally developed to provide hazard by manipulating local seismic histories and only using epicentral data to fill informative gaps eventually due to the lack of documentation. In this preliminary application to Iran, however, the lack of a detailed historical reconstruction of local seismic histories, required the application of the SASHA approach to local seismic histories reconstructed from epicentral information by the use of attenuation relationship. In this regard, the present application should be seen as first approach stimulating new historical studies relative to the local effects of past earthquakes.

In principle, SASHA is a distribution-free approach as it does not assume any specific distribution of seismicity rates, and it does not require removal of aftershocks. However, in regions like Iran where comprehensive site-specific seismic histories are lacking, reliance on a probabilistic attenuation relationship becomes necessary. In the case of Iran, a maximum likelihood analysis was conducted to select the best-performing attenuation relationship by considering seismic histories at a set of sites. It should be noted that the current application of SASHA in Iran does not fully exploit the potential of the approach due to the lack of extensive records of locally felt intensity, as seen in countries like Italy.

Nevertheless, since SASHA outcomes strictly represent the contribution of historical seismicity to seismic hazard, they serve as a baseline for hazard assessment and a useful benchmark for more advanced estimates developed using complex approaches that also consider seismotectonic zonings in addition to earthquake statistics.

A comparison of ranks between SASHA estimates and those provided by Hosseini Varzandeh and Mahsuli (2023a) for Iran indicates significant differences. For instance, Tehran exhibits a relatively low seismic hazard, with an intensity level reaching only VI and a 10% exceedance probability within 50 years, despite the proximity to major fault lines. This is supported by the observation that no medium- to large-magnitude earthquakes (Mw 6.5–7.5) have occurred in the Tehran metropolitan area over the past 839 years, indicating low seismic activity rates. However, paleo-seismological research indicates that the North Tehran, Taleghan, and Mosha faults have experienced significant seismic events in the distant past, suggesting longer recurrence intervals and potential seismic threats. Several factors could explain these differences, including challenges in parameterizing historical earthquakes and assessing intensity, as well as the incompleteness of the historical record. However, these challenges also affect standard approaches, as historical events still play a major role in hazard assessment. To mitigate these issues, geological data can be considered for identifying seismogenic structures, although the actual seismogenic capability of identified structures may be uncertain.

The aim of this comparison is not to validate one approach over the other, and the results obtained by SASHA do not imply that hazard estimates by Hosseini Varzandeh and Mahsuli (2023a) are incorrect. Instead, this comparison can inform more detailed analyses where potential drawbacks or advantages of both approaches are carefully examined on a case-by-case basis. Additionally, this comparison can help identify critical situations that warrant further study, both from historical and seismotectonic perspectives, to provide more effective and robust hazard estimates in the future.

Supplementary Information The online version contains supplementary material available at <https://doi.org/10.1007/s10518-024-01960-7>.

Author contribution All authors contributed to the study conception and design. Material preparation, data collection and analysis were performed by all Authors. The first draft of the manuscript was written by ES and DA and all authors commented on previous versions of the manuscript. All authors read and approved the final manuscript.

Funding Open access funding provided by Università degli Studi di Siena within the CRUI-CARE Agreement.

Declarations

Conflict of interest The authors declare that no funds, grants, or other support were received during the preparation of this manuscript. The authors have no relevant financial or non-financial interests to disclose.

Open Access This article is licensed under a Creative Commons Attribution 4.0 International License, which permits use, sharing, adaptation, distribution and reproduction in any medium or format, as long as you give appropriate credit to the original author(s) and the source, provide a link to the Creative Commons licence, and indicate if changes were made. The images or other third party material in this article are included in the article's Creative Commons licence, unless indicated otherwise in a credit line to the material. If material is not included in the article's Creative Commons licence and your intended use is not permitted by statutory regulation or exceeds the permitted use, you will need to obtain permission directly from the copyright holder. To view a copy of this licence, visit <http://creativecommons.org/licenses/by/4.0/>.

References

- Abbasi S, Motaghi K, Lucente FP, Bianchi I (2024) Low-strength shear zone in the western Makran subduction zone, southeastern Iran: insights from a receiver function analysis. *Geophys J Int* 237(1):64–74
- Aghdam MA, Ghods A, Sobouti F, Motaghi K, Priestley K, Enayat M (2024) Seismicity around the boundary between eastern and western Makran. *J Asian Earth Sci* 259:105926
- Aguado JLP, Ferreira TM, Lourenco PB (2018) The use of a large-scale seismic vulnerability assessment approach for masonry façade walls as an effective tool for evaluating, managing and mitigating seismic risk in historical centers. *Int J Archit Herit* 12(7–8):1259–1275
- Ahmadzadeh S, Javan Doloei G, Zafarani H (2019) New intensity prediction equation for Iran. *J Seismol* 24(6):23–35. <https://doi.org/10.1007/s10950-019-09882-7>
- Albarelo D (2012) Design earthquake from site-oriented macroseismic hazard estimates. *Boll Geofis Teor Appl* 53(1):7–17. <https://doi.org/10.4430/bgta0035>
- Albarelo D, Camassi R, Rebez A (2001) Detection of space and time heterogeneity in the completeness of a seismic catalog by a statistical approach: an application to the Italian area. *Bull Seismol Soc Am* 91(6):1694–1703
- Ambraseys NN (2001) Reassessment of earthquakes, 1900–1999, in the eastern Mediterranean and the Middle East. *Geophys J Int* 145:471–485
- Ambraseys NN, Melville CP (1982) A history of persian earthquake. Cambridge University Press, Cambridge
- Amini H, Zare M, Gasperini P (2017) Re-assessing the intensity values of Iranian earthquakes using EMS and ESI scales. *Arab J Geosci* 10:504. <https://doi.org/10.1007/s12517-017-3226-3>
- Arsilan Kelam A, Karimzadeh S, Yousefibaivil K, Akgün H, Askan A, Erberik MA, Koçkar MK, Pekcan O, Ciftci H (2022) An evaluation of seismic hazard and potential damage in Gaziantep, Turkey using site specific models for sources, velocity structure and building stock. *Soil Dyn Earthq Eng* 154:107129
- Askari M, Mahsuli M (2020) Modeling of epistemic uncertainties in seismic hazard analysis based on reliability methods. In: Technical report, center for infrastructure sustainability and resilience research, Sharif University of Technology; Tehran, Iran.
- Berberian M (1976a) Documented earthquake faults in Iran. *Geol Surv Iran* 39:143–186
- Berberian M (1976b) Quaternary faults in Iran. *Geol Surv Iran* 39:187–258
- Berberian M (1976c) Contribution of the seismotectonics of Iran (Part II). Geological and mining survey of Iran, Report No. 39.
- Berberian M (1977) Contribution of the seismotectonics of Iran (Part III). Geological and mining survey of Iran, Report No. 40.
- Berberian M (1981) Active faulting and tectonics of Iran. In: Gupta HK, Delany FM (eds) Zagros-Hindu Kush-himalaya geodynamic evolution. American Geophysical Union, Geodynamics Series Volume 3, American Geophysical Union, pp 33–69
- Berberian M (2005) The 2003 Bam urban earthquake: a predictable seismotectonic pattern along the western margin of the rigid Lut Block. *Southeast Iran Earthq Spectra* 21(S1):S35–S99
- Berberian M, Yeats RS (2016) Tehran: an earthquake time bomb. In: Sorkhabi R (ed.) Tectonic evolution, collision, and seismicity of Southwest Asia: in honor of manuel Berberian's forty-five years of research contributions. Geological Society of America Special Paper 525, p. 1–84. [https://doi.org/10.1130/2016.2525\(04\)](https://doi.org/10.1130/2016.2525(04))
- Berberian M, Jackson JA, Fielding E, Parsons BE, Priestley K, Qorashi M, Talebian M, Walker R, Wright TJ, Baker C (2001) The 1998 March 14 Fandoqa earthquake (Mw 6.6) in Kerman province, southeast Iran: re-rupture of the 1981 Sirch earthquake fault, triggering of slip on adjacent thrusts and the active tectonics of the Gowk fault zone. *Geophys J Int* 146:371–398
- Bindi D, Abdrakhmatov K, Parolai S et al (2012) Seismic hazard assessment in Central Asia: outcomes from a site approach. *Soil Dyn Earthq Eng* 37:84–91
- Byrne DE, Sykes LR, Davis DM (1992) Great thrust earthquakes and aseismic slip along the plate boundary of the Makran Subduction Zone. *J Geophys Res* 97:449–478. <https://doi.org/10.1029/91JB02165>
- Chandra U, McWhorter JG, Nowroozi AA (1979) Attenuation of intensities in Iran. *Bull Seismol Soc Am* 69(1):237–250
- Chieffo N, Formisano A, Ferreira TM (2019) Damage scenario-based approach and retrofitting strategies for seismic risk mitigation: an application to the historical Centre of Sant'Antimo (Italy). *Eur J Env Civ Eng* 25(11):1929–1948
- D'Amico V, Albarelo D (2008) SASHA: a computer program to assess seismic hazard from intensity data. *Seismol Res Lett* 79(5):663–671

- D'Amico V, Albarello D, Sigbjörnsson R, Rupakhety R (2016) Seismic hazard assessment for Iceland in terms of macroseismic intensity using a site approach. *Bull Earthq Eng* 14:1797–1811
- Del Gaudio C, De Martino G, Di Ludovico M, Manfredi G, Prota A, Ricci P, Verderame GM (2019) Empirical fragility curves for masonry buildings after the 2009 L'Aquila, Italy, earthquake. *Bull Earthq Eng* 17:6301–6330
- Di Pasquale G, Orsini G, Romeo RW (2005) New developments in seismic risk assessment in Italy. *Bull Earthq Eng* 3(1):101–128
- Dumova-Jovanoska E (2000) Fragility curves for reinforced concrete structures in Skopje (Macedonia) region. *Soil Dyn Earthq Eng* 19:455–466
- Fragiadakis M, Diamantopoulos S (2020) Fragility and risk assessment of freestanding building contents. *Earthq Eng Struct Dyn* 49:1028–1048. <https://doi.org/10.1002/eqe.3276>
- Gómez Capera AA, D'Amico V, Meletti C, Rovida A, Albarello D (2010) Seismic hazard assessment in terms of macroseismic intensity in Italy: a critical analysis from the comparison of different computational procedures. *Bull Seismol Soc Am* 100(4):1614–1631
- Gómez Capera AA, D'Amico M, Lanzano G, Locati M, Santulin M (2020) Relationships between ground motion parameters and macroseismic intensity for Italy. *Bull Earthq Eng* 18:5143–5164
- Grünthal G (1998) European Macroseismic Scale 1998, Cahiers du Centre Européen de Géodynamique et de Seismologie 15. Conseil de l'Europe, pp 99
- Guerrieri L, Michetti AM, Reicherter K, Serva L, Silva PG, Audemard F, Azuma T, Baiocco F, Baize S, Blumetti AM, Brustia E, Clague J, Commerci V, Esposito E, Gurpinar A, Grutzner C, Jin K, Kim YS, Kopsachilis V, Lucarini M, McCalpin J, Mohammadioun B, Morner NA, Okumura K, Ota Y, Papatthanassiou G, Pavlides S, López Perez, Porfido R, Rodríguez Pascua S, Rogozhin MA, Scaramella E, Sintubin A, Tatevossian M, Vittori E, (2015) Earthquake environmental effect for seismic hazard assessment: the ESI intensity scale and the EEE Catalogue. *Memorie Descrittive Della Carta Geologica d'Italia V*, pp. XC VII
- Hessami K, Jamali F, Abasi H (2003) Major Active Faults of Iran. International Institute of Earthquake Engineering and Seismology (IIEES), Arghavan
- Hosseini Varzandeh S, Mahsuli M (2023a) Probabilistic framework for robust optimal code calibration through minimization of the lifecycle cost and its uncertainty. *Bull Earthq Eng*. <https://doi.org/10.1007/s10518-023-01816-6>
- Hosseini Varzandeh S, Mahsuli M (2023b) Codified robust optimal design base shear of structures: Methodology and application to reinforced concrete buildings. *Soil Dyn Earthq Eng* 174:108200. <https://doi.org/10.1016/j.soildyn.2023.108200>
- Jena R, Pradhan B, Beydoun G, Al-Amri A, Sofyan H (2020) Seismic hazard and risk assessment: a review of state-of-the-art traditional and GIS models. *Arab J Geosci*. <https://doi.org/10.1007/s12517-019-5012-x>
- Jimenez M-J, Albarello D, Garcia-Fernandez M (2016) PSHA in SE Spain based on macroseismic site histories. *Bull Earthq Eng* 14:1849–1867. <https://doi.org/10.1007/s10518-015-9784-4>
- Lagomarsino S, Giovinazzi S (2006) Macroseismic and mechanical models for the vulnerability and damage assessment of current buildings. *Bull Earthq Eng* 4(4):415–443
- Mahsuli M, Rahimi H, Bakhshi A (2019) Probabilistic seismic hazard analysis of Iran using reliability methods. *Bull Earthq Eng* 17:1117–1143. <https://doi.org/10.1007/s10518-018-0498-2>
- Martins L, Silva V (2021) Development of a fragility and vulnerability model for global seismic risk analyses. *Bull Earthq Eng* 19:6719–6745. <https://doi.org/10.1007/s10518-020-00885-1>
- Mirzaei N, Gao M, Chen YT (1998) Seismic source regionalization for seismic zoning of Iran: major seismotectonic provinces. *J Earthqu Pred Res* 7:465–495
- Moradi A, Mirzaei N, Rezapour M (2004) The attenuation of seismic intensity in Iran (in Persian). *J Earth Space Phys* 30(1):1–9
- Mousavi Bafrouei SH, Mahani AB (2020) A comprehensive earthquake catalogue for the Iranian Plateau (400 B.C. to December 31, 2018). *J Seismol* 24:709–724. <https://doi.org/10.1007/s10950-020-09923-6>
- Mousavi Bafrouei SH, Mirzaei N, Shabani E, Eskandari-Ghadi M (2014) Seismic hazard zoning in Iran and estimating peak ground acceleration in provincial capitals. *J Earth Space Phys* 40(4):15–38
- Mucciarelli M, Albarello D, D'Amico V (2008) Comparison of Probabilistic Seismic Hazard estimates in Italy. *Bull Seism Soc Am* 98(6):2652–2664. <https://doi.org/10.1785/0120080077>
- Musson RM, Grünthal G, Stucchi M (2010) The comparison of macroseismic intensity scales. *J Seismol* 14:413–428
- Penney C, Tavakoli F, Saadat A, Nankali HR, Sedighi M, Khorrami F, Sobouti F, Rafi Z, Copley A, Jackson J, Priestley K (2017) Megathrust and accretionary wedge properties and behaviour in the Makran subduction zone. *Geophys J Int* 209(3):1800–1830

- Rahimi H, Mahsuli M (2019) Structural reliability approach to analysis of probabilistic seismic hazard and its sensitivities. *Bull Earthq Eng* 17(3):1331–1359. <https://doi.org/10.1007/s10518-018-0497-3>
- Ritz JF, Nazari H, Ghassemi A, Salamati R, Shafei A, Solaymani S, Vernant P (2006) Active transtension inside Central Alborz: a new insight of the Northern Iran-Southern Caspian geodynamics. *Geology* 34:477–480. <https://doi.org/10.1130/G22319.1>
- Ritz JF, Nazari H, Balescu S, Lamothe M, Salamati R et al (2012) Paleoearthquakes of the past 30,000 years along the North Tehran Fault (Iran). *J Geophys Res* 117:B06305
- Salditch L, Gallahue MM, Stein S, Neely JS, Abrahamson N, Hough SE (2024) Why do seismic hazard models worldwide appear to overpredict historical intensity observations? *Sci Adv* 10:eadj9291
- Saunders JK, Minson SE, Baltay AS (2022) How low should we alert? Quantifying intensity threshold alerting strategies for earthquake early warning in the United States. *Earth's Future* 10:e2021EF002515
- Shedlock KM, Giardini D, Grünthal G, Zhang P (2000) The GSHAP global seismic hazard map. *Seism Res Lett* 71(6):679–689
- Ullah S, Bindi D, Pilz M, Danciu L, Weatherill G, Zuccolo E, Ischuk A, Mikhailova NN, Abdrakhmatov K, Parolai S (2015) Probabilistic seismic hazard assessment for Central Asia. *Ann Geophys.* <https://doi.org/10.4401/ag-6687>
- Wieland M, Pittore M, Parolai S, Zschau J (2012) Exposure estimation from multi-resolution optical satellite imagery for seismic risk assessment. *ISPRS Int. J. Geo-Inf.* 1(1):69–88. <https://doi.org/10.3390/ijgi1010069>
- Yaghmaei-Sabegh S (2018) Macroseismic intensity attenuation in Iran. *Earthq Eng Vib* 17:139–148. <https://doi.org/10.1007/s11803-018-0430-4>
- Zare M (2017) Recent development of the earthquake strong motion-intensity Catalog and intensity prediction equations for Iran. *J Seismol.* <https://doi.org/10.1007/s10950-016-9622>

Publisher's Note Springer Nature remains neutral with regard to jurisdictional claims in published maps and institutional affiliations.